Utilization of Glycerol for Endogenous Glucose and Glycogen Synthesis in Juvenile Seabass: a Novel Mechanism for Sparing Amino Acid Catabolism in Carnivorous Fish

Joao Rito[a,b,c], Ivan Viegas[a,b,c], Miguel Â. Pardal[b,c], Isidoro Metón[d], Isabel V. Baanante[d], and John G. Jones[a,c*]

[a]CNC - Center for Neurosciences and Cell Biology, University of Coimbra, 3004-517 Coimbra, Portugal.

[b]CFE - Center for Functional Ecology, University of Coimbra, Apartado 3046, 3001-401 Coimbra, Portugal.

[c]Department of Life Sciences, University of Coimbra, 3001-401 Coimbra, Portugal.

[d]Secció de Bioquímica i Biologia Molecular, Departament de Bioquímica i Fisiologia, Facultat de Farmàcia, Universitat de Barcelona, Joan XXIII 27, 08028 Barcelona, Spain.

***Address for Correspondence:**

John G. Jones, D.Sc.

Center for Neurosciences and Cell Biology

UC Biotech, Biocant Park,

Nucleo 4, Lote 8, 3060-197 Cantanhede, Portugal

email: john.griffith.jones@gmail.com

Keywords: ^{13}C NMR isotopomer analysis, gluconeogenesis, triose phosphate isomerase, glycerol kinase

Abstract

Glycerol is a well-tolerated additive in aquafeeds. We hypothesized that in seabass, a carnivorous fish whose endogenous carbohydrate demands are mostly met by hepatic amino acid gluconeogenesis, glycerol effectively competes with these substrates for endogenous glucose and glycogen synthesis. To test this hypothesis, we injected fasted and fed juvenile seabass with an intraperitoneal 2 g.kg-1 bolus of glycerol enriched to 25% with [U-$^{13}C_3$]glycerol and monitored the appearance of blood glucose and hepatic glycogen ^{13}C-isotopomers 48-hours thereafter by ^{13}C NMR spectroscopy. This information was used to determine the fractional contribution of the glycerol load to systemic glucose appearance and liver glycogen synthesis. In 21-day fasted fish, the glycerol bolus contributed 47 ± 3% of circulating glucose appearance and 40 ± 3% of hepatic glycogen at 48-hr post-bolus. In fed fish, the glycerol bolus accounted for 17 ± 3% of circulating glucose and 3 ± 1% of hepatic glycogen at 48-hr post-polus. While the majority of glycerol was metabolized to glucose and glycogen via the canonical linear gluconeogenic pathway, a significant minority was converted to glucose and glycogen via the hepatic Krebs cycle. In fasted fish, linear gluconeogenesis accounted for 40 ± 3% of glucose appearance while the Krebs cycle route accounted for 7 ± 2%. In fed fish, linear and Krebs cycle-mediated contributions were 10 ± 2% and 6 ± 2%, respectively. These data indicate that glycerol effectively competes with endogenous precursors for hepatic gluconeogenesis in carnivorous fish thereby representing a novel mechanism for reducing the catabolic utilization of amino acids.

1. Introduction:

The European seabass (*Dicentrarchus labrax*) is a carnivorous fish that is widely cultured in Europe (FEAP, 2017). It is adapted to a diet high in protein (Peres and Oliva-Teles 1999) hence its hepatic intermediary metabolism is characterized by high rates of catabolic amino acid (AA) utilization for the biosynthesis of carbohydrates and for energy generation. In addition to diverting AA away from

muscle growth, these processes generate waste ammonia (Peres and Oliva-Teles 2005). Thus, there is strong interest in identifying feed supplements that not only replace dietary protein but also attenuate AA catabolism. AA-gluconeogenesis is a central pathway for synthesis of hepatic glucose-6-phosphate (Glc-6-P) - the principal precursor for the synthesis of endogenous glucose, glycogen and the carbohydrate moieties of glycoproteins and other structural carbohydrate components (Hers 1976; Krebs 1964). Therefore, substrates that compete with AA for Glc-6-P synthesis could in principle be effective at sparing gluconeogenic AA catabolism.

Glycerol is one such substrate that can potentially compete with gluconeogenic AA for hepatic Glc-6-P synthesis. Following the growth in biodiesel production there is now a worldwide abundance of glycerol and it has been tested as a feed supplement for various farmed animals, including fish (Arif et al. 2017; Lee et al. 2011; Li et al. 2010; Meurer et al. 2012; Moesch et al. 2016). To date, studies have shown that glycerol supplementation up to 15% of total feed does not impair growth rates or feed conversion ratios in several different fish species (da Costa et al. 2017; Gonçalves et al. 2013; Li et al. 2010; Silva et al. 2012). However, while there have been a few studies of glycerol metabolism in various fish species, its contribution to endogenous carbohydrate synthesis has not been specifically determined. In mammals, a glycerol load is rapidly and efficiently converted to glucose and glycogen via hepatic gluconeogenesis and glycogenesis (Kosuga et al. 2011; Lin 1977). Such activity has not been generally well described in fish species, although early *in vitro* studies of rainbow trout (*Oncorhynchus mykiss*) liver slices reported a capacity for glycerol conversion to glycogen by carnivorous fish (Lech 1970). A recent study of [U-^{14}C]glycerol utilization by Nile tilapia (*Oreochromis niloticus*) revealed that the major fraction of the label was recovered in liver and muscle tissue fractions that were not protein or lipid (da Costa et al. 2017). Therefore, our aim was to assess the capacity of juvenile seabass to incorporate glycerol carbons into endogenous circulating glucose and hepatic glycogen following an intraperitoneal injection of glycerol. Glycerol incorporation was primarily measured by quantifying the appearance of glucose

and glycogen ^{13}C-isotopomers from a glycerol load enriched with [U-$^{13}C_3$]glycerol. Our data showed that juvenile seabass have an inherently strong capacity for converting glycerol to both glucose and glycogen appearances and in doing so displaces contributions from gluconeogenic AA.

2. Materials and Methods

2.1 Fish handling: For this experiment, 80 European seabass (*Dicentrarchus labrax* L.) provided by a local farm were transported to the lab and randomly distributed in four tanks of 200 L volume capacity. There were 20 fish per tank with a mean initial body weight of 48 ± 3 g and a mean initial body length of 15.4 ± 0.3 cm. Fish were acclimated for one month in a recirculating aquatic system (RAS) equipped with a central filter and UV unit at 20ºC temperature, 30‰ salinity and well aerated seawater (> 90% O2). Water temperature, pH, dissolved oxygen and salinity were continuously monitored and NH_4^+, NO_3^- and NO_2^- were measured twice weekly and were found to be within optimal ranges. During the acclimation period fish were fed every day with automated feeders to satiety (feeders distributed four to six meals per day, with the meal size and the number of meals adjusted based on the presence of uneaten feed in the tank) with a commercial diet (Aquagold 5, SORGAL, S.A.; 45.0% crude protein, 18.0% fat, 10.0% ash, 2.0% fiber, 2.0% calcium, 1.0% phosphorus, 0.4% sodium, 19% nitrogen-free extract). After acclimation, two groups of fish were fasted for 21 days while the others were maintained on the described feeding protocol.

2.2 Glycerol injection and sampling: At the end of the feeding/fasting period, fish were anesthetized in a 30 L tank containing the same rearing seawater with 0.1 $g.L^{-1}$ of MS-222. They were then measured, weighed, and 100 µL of blood was taken with heparinized syringes from the caudal vein and kept on ice until processing. An intraperitoneal injection was given to each fish (10 $mL.kg^{-1}$) of 200 $mg.ml^{-1}$ of glycerol enriched to 25% with [U-$^{13}C_3$]glycerol for a load of 2 $g.kg^{-1}$. The second groups of fish serving as controls were injected with an equivalent volume of saline. Fish were

allowed to recover in the same rearing seawater and were not fed for the following 48 hours. After the 48 hours, fish were again anesthetized, measured and weighed. Blood was collected and an aliquot of 100 µL was kept for glucose and glycerol assays with the remaining portion kept for glucose derivatization and ^{13}C NMR analysis. Fish were then sacrificed by cervical section. Livers were extracted and freeze clamped under liquid nitrogen and then stored at -80ºC until further processing. All these procedures complied with the Guidelines of the European Union Council (86/609/EU).

2.3 Sample processing: Blood aliquots of 100 µL were centrifuged at 3000 g for 10 min and plasma was collected and stored at -20°C. Plasma glucose and glycerol levels were measured with commercial kits (Amplex® Red Glucose/Glucose Oxidase Assay Kit, Invitrogen; Glycerol Assay Kit, Sigma-Aldrich Co. LLC). Blood from 2-3 fish was pooled for ^{13}C-NMR isotopomer analysis of glucose enrichment. Blood samples were deproteinized by adding 0.3 M $ZnSO_4$ and 1.5 M $Ba(OH)_2$ (1.5 mL of each per mL of blood) and centrifuged at 3500 g for 15 min. The supernatant was desalted by passage through sequential columns containing Dowex® 50WX8 (hydrogen form; Sigma-Aldrich) and Amberlite® IRA-67 (free base, Fluka; Sigma-Aldrich) and the column effluents were lyophilized. For quantification and ^{13}C NMR isotopomer analysis of hepatic glycogen, livers from 2 fish were pooled and glycogen extraction, quantification and hydrolysis to glucose was performed according to Viegas et al. (Viegas et al. 2012). Glycogen was extracted by alcoholic precipitation after alkaline tissue hydrolysis following Good et al. (1933) (Good et al. 1933). Briefly, powder frozen liver was treated with 30% KOH (2 mL per gram of liver) at 70°C for 30min. After vigorous vortex, the mixture was treated with 6% Na2SO4 (1 mL per gram of liver) and 99.9% ethanol (to a final concentration of 70%, 7 mL per gram of liver) and left overnight at 4 °C to precipitate glycogen. After centrifugation, the upper liquid phase was discarded and the solid residue dried. The residue was resuspended in 5 mL acetate buffer (0.05 M pH = 4.5), and 20 µL of an

aqueous solution containing 16 U of amyloglucosidase from *Aspergillus niger* (Glucose-free preparation, Sigma-Aldrich, Germany) was added to hydrolyse glycogen to its glucosyl units. Samples were incubated overnight at 55°C and centrifuged. The supernatant was collected and a 100 µL aliquot was stored separately. The glucose derived from glycogen enzymatic hydrolysis was quantified by assay kit (Amplex® Red Glucose/Glucose Oxidase Assay Kit, Invitrogen).

Glucose samples obtained from blood and liver glycogen were then derivatized to monoacetone glucose (MAG) (Viegas et al. 2012). MAG was further purified by solid phase extraction and prepared for ^{13}C NMR spectroscopy as recently described (Rito et al. 2017).

2.4 ^{13}C NMR Spectroscopy: Proton-decoupled ^{13}C NMR spectra of MAG were acquired at 14.1 T with a Varian VNMRS 600 MHz NMR (Agilent, Santa Clara, CA, USA) spectrometer equipped with a 3 mm broadband probe with z-gradient. Spectra were obtained at a temperature of 25ºC, using a 70° pulse, 2.5 s acquisition time, 0.5 s pulse delay and 5,000 to 15,000 free-induction decays (f.i.d.). The two methyl naturalabundance carbon signals of MAG were used as intramolecular standards for converting the ^{13}C isotopomer multiplet areas of carbon 2 and carbon 5 into ^{13}C-isotopomer enrichment values for [1,2,3-$^{13}C_3$]hexose, [4,5,6-$^{13}C_3$]hexose, [1,2-$^{13}C_2$]hexose, [5,6-$^{13}C_2$]hexose, [2,3-$^{13}C_2$]hexose and [4,5-$^{13}C_2$]hexose. Isotopomer signals were defined to be below the limits of quantification when their signal-to-noise ratio was below 5:1. NMR spectra were analyzed with ACD/NMR Processor Academic Edition software (ACD/Labs, Advanced Chemistry Development, Inc.).

*2.5 Theory and metabolic flux calculations***:**

As shown in Figure 1, direct gluconeogenic conversion of [1,2,3-$^{13}C_3$]glycerol to Glc-6-P results in the formation of [1,2,3-$^{13}C_3$] and [4,5,6-$^{13}C_3$]hexose isotopomers. This mixture is hereafter referred to as isotopomers **A**. If [1,2,3-$^{13}C_3$]glycerol is metabolized to Glc-6-P via the Krebs cycle, a

proportion is converted to [2,3-$^{13}C_2$]Triose-P due to label randomization by the exchange of oxaloacetate, malate and fumarate. These [2,3-$^{13}C_2$]Triose-P intermediates are metabolized via gluconeogenesis to form [1,2-$^{13}C_2$] and [5,6-$^{13}C_2$]Glc-6-P, hereafter referred to as isotopomers **B**. Assuming that Krebs cycle randomization is complete, each equivalent of [1,2,3-$^{13}C_3$] or [4,5,6-$^{13}C_3$]glycerol that is metabolized via the Krebs cycle generates 0.5 equivalents of [1,2-$^{13}C_2$] or [5,6-$^{13}C_2$]hexose and 0.5 equivalents of [1,2,3-$^{13}C_3$] or [4,5,6-$^{13}C_3$]hexose. Therefore, the linear gluconeogenic pathway contribution is estimated by the difference between isotopomers **A** and **B** enrichments, as shown below:

Linear gluconeogenesis (%) = [Isotopomers **A** (%) – Isotopomers **B** (%)] × 100/F (**1**)

Where isotopomers **A** represent the mean abundance of [1,2,3-$^{13}C_3$] and [4,5,6-$^{13}C_3$]hexose isotopomers, isotopomers **B** represent the mean abundance of [1,2-$^{13}C_2$] and [5,6-$^{13}C_2$]hexose isotopomers, and F is the percent fractional enrichment of the glycerol load.

The contribution of gluconeogenesis via the Krebs cycle was estimated by the following equation:

Krebs cycle gluconeogenesis (%) = 2 × Isotopomers **B** × 1.5 × 100/F (**2**)

Multiplication by 2 reflects the fact that isotopomers **B** are accompanied by equivalent amounts of isotopomers **A**. In the Krebs cycle, there is dilution of both **A** and **B** isotopomer populations by unlabeled oxaloacetate that is formed via the oxidative portion of the cycle. The dilution factor of 1.5 is based on the assumption of net anaplerotic flux being twice that of oxidative Krebs cycle flux (Rito et al, 2017).

2.6 Statistical analysis:

Values are expressed as means ± standard error of the mean (S.E.M.). Statistical differences between groups with $P < 0.05$ were assessed using Student's two-tailed unpaired *t* test.

3. Results:

3.1 Circulating metabolites and hepatic glycogen: The effects of the intraperitoneal glycerol injection on selected metabolites of interest were evaluated. Plasma glucose levels in fasted seabass, while showing high variability between individual fish, tended to increase following the glycerol load (Table 1). Plasma glucose levels of fed fish showed no discernible effects from glycerol injection (Table 1). Hepatic glycogen levels were not statistically different between fasted and fed fish at 48 hr following the glycerol load (Table 1). However, they showed statistical differences between fasted and fed fish in the control groups ($P<0.001$) and between fasted fish in the control group and fasted fish 48-hour postglycerol load ($P<0.005$) (Table 1).

3.2 NMR analysis of gluconeogenic [U-^{13}C]glycerol metabolism: Passage of ^{13}C from the injected [U-^{13}C]glycerol into endogenous glucose and glycogen was monitored by ^{13}C NMR. Figure 2 shows ^{1}H NMR spectra of plasma following deproteinization and derivatization of the glucose to MAG for fasted and fed fish that received the glycerol load (Fig. 2a) and the corresponding controls that received saline (Fig. 2b). Fish that received the glycerol load showed additional signals attributable to glycerol that had comparable intensities to those of MAG while saline-injected controls had residual amounts of glycerol signals. The ^{1}H NMR resonances of MAG derived from plasma glucose of the glycerol-injected fish showed characteristic satellite signals originating from ^{1}H-^{13}C coupling indicating enrichment by ^{13}C. This is most clearly observed for the well-resolved resonance of the hydrogen bound to carbon 1.

Figure 3 shows the corresponding ^{13}C NMR spectra obtained from these samples. For the fish that did not receive [U-$^{13}C_3$]glycerol, represented by Figure 3b, the spectra consist of singlet signals representing the 1.11% natural abundance ^{13}C-enrichment. Differences in ^{13}C-signal amplitudes, for example carbon 1 *versus* carbon 2, reflect differences in ^{13}C-signal linewidths between different positions. Within the limits of precision determined by the signal-to-noise ratio, the relative areas of the six hexose and two acetonide signals were equivalent. For the fish that received the [U-$^{13}C_3$]glycerol load, the singlet natural-abundance signals for the six hexose carbons were accompanied by multiplets representing glucose ^{13}C-isotopomers formed by conversion of [U-$^{13}C_3$]glycerol to glucose. The multiplet structures originate from the splitting of the ^{13}C-signal by ^{13}C-^{13}C-coupling with a neighbouring ^{13}C nucleus. Also present are singlet and multiplet signals originating from circulating glycerol derived from the [U-$^{13}C_3$]glycerol-enriched load. Multiplets of the carbon 2 and carbon 5 ^{13}C NMR signals, shown in expanded form, provide quantitative information on the appearance of glucose and glycogen ^{13}C-isotopomers **A-D** derived from the [U-$^{13}C_3$]glycerol load. ^{13}C-Isotopomer abundances from the de-convolution and analysis of these multiplets are shown in Table 2.

Figure 4 shows the carbon 2 multiplets of MAG derived from blood glucose and liver glycogen from a fasted and a fed seabass administered with [U-$^{13}C_3$]glycerol. Up to nine peaks can be observed: a quartet component (**C2Q**) representing [1,2,3-$^{13}C_3$]hexose formed by the gluconeogenic conversion of [U-$^{13}C_3$]glycerol to glucose via triose and hexose phosphates; a doublet (**C2D12**) representing [1,2-$^{13}C_2$]hexose formed by the cycling of [1,2,3-$^{13}C_3$]triose-P via pyruvate and the Krebs cycle; a minor doublet (**C2D23**) representing [2,3-$^{13}C_2$]hexose formed by further randomization of label through a full turn of the Krebs cycle, and a singlet (**C2S**) representing the natural-abundance ^{13}C from triose moieties that were not derived from [U-$^{13}C_3$]glycerol. The carbon 5 multiplet yielded information for the corresponding [4,5,6-$^{13}C_3$], [5,6-$^{13}C_2$] and [4,5-$^{13}C_2$]hexose

isotopomers from the other triose half of glucose (not shown). The calculated isotopomer abundances from analysis of the ^{13}C NMR carbon 2 and carbon 5 multiplets are shown in Table 2.

For fasted fish, the glucose multiplet was dominated by **C2Q**, representing [1,2,3-$^{13}C_3$]glucose and reflecting high incorporation of [U-$^{13}C_3$]glycerol into glucose via the linear gluconeogenic pathway. However, the presence of **C2D12** signals, representing [1,2-$^{13}C_2$]glucose, indicates that a portion of glycerol carbons were metabolized to hexose via the Krebs cycle. The low abundance of [1,2-$^{13}C_2$]glucose relative to [1,2,3-$^{13}C_3$]glucose (similarly [5,6-$^{13}C_2$]glucose relative to [4,5,6-$^{13}C_3$]glucose) indicates that the majority of glycerol carbons were converted to glucose via the linear gluconeogenic pathway. ^{13}C NMR spectra of MAG derived from liver glycogen had substantially higher signal-to-noise ratio compared to that of the blood because of the higher quantities of glucosyl units that were recovered from the pooled liver glycogen samples.

Glycogen and glucose ^{13}C-isotopomers from fasted fish showed similar but not identical ^{13}C-isotopomer populations. The singlet component was noticeable higher in spectra derived from glycogen compared to those from glucose. This can be attributed to the presence of pre-existing unlabeled glycogen resulting from incomplete turnover of the hepatic glycogen pool during the 48-hour period of tracer administration. This fraction only contributes to the ^{13}C-natural-abundance singlet signals thereby increasing its intensity relative to the multiplets derived from glycogen that was synthesized from [U-$^{13}C_3$]glycerol. Based on previous estimates of glucose turnover in Kelp bass (Bever et al. 1977), the whole-body glucose pool is assumed to have been fully replaced during this period hence there is no pre-existing glucose that would selectively contribute to the natural-abundance singlet signals. While levels of isotopomers **A** were similar for plasma glucose and glycogen of fasted fish (see Table 2), the abundances of isotopomers **B** were higher in glycogen compared to glucose.

Plasma glucose ^{13}C NMR multiplets from fed fish showed substantial differences from those of fasted fish, as exemplified by the carbon 2 multiplets shown in Figure 4. The **C2Q** contribution was

substantially lower compared to the fasting condition indicating a lower fractional contribution of linear glycerol gluconeogenesis to plasma glucose appearance. The **C2D12** signal intensity was similar to that of fasted fish, indicating that glycerol metabolism to glucose via the Krebs cycle contributed a similar fraction of glucose appearance. The **C2D23** signals were below the limit of quantification suggesting that the fraction of glycerol carbons that underwent a complete Krebs cycle turn before being reincorporated into gluconeogenesis was also reduced. As shown in Table 2, differences in carbon 5 isotopomer abundances between fed and fasted fish were fairly consistent with those of carbon 2. ^{13}C-Glycogen signals from fed fish were dominated by the natural abundance singlet signal from pre-existing glycogen. The very low intensities of the multiplet signals relative to the singlet (see Table 2) indicates that only a minor fraction of liver glycogen was derived from the [U-$^{13}C_3$]glycerol load under these conditions.

3.3 Conversion of the glycerol load to circulating glucose and hepatic glycogen: From the ^{13}C-isotopomer analyses of glucose and glycogen, estimates for the fractional contribution of the glycerol load to these metabolites via the canonical gluconeogenic pathway involving triose phosphate intermediates and by a more circuitous route involving initial conversion to pyruvate followed by triose phosphate regeneration via Krebs cycle anaplerosis. Table 3 shows estimates of the glycerol fractional contribution to glucose and glycogen appearance. Under fasting conditions, the glycerol load accounted for almost one-half of glucose appearance at 48 hours post-injection. The majority of glycerol carbons were converted to glucose via the linear gluconeogenic pathway while glycerol conversion to glucose via pyruvate and the Krebs cycle accounted for a minor fraction. Analysis of glycogen ^{13}C-isotopomers showed that approximately 40% of total glycogen was derived from glycerol. In comparison to plasma glucose the fractional contribution of the linear pathway was lower and contributions via the Krebs cycle were higher. In fed fish, the contribution of the glycerol load to plasma glucose appearance was more modest, with linear gluconeogenesis contributing about

twice that of the Krebs cycle pathway. The contribution of the glycerol load to liver glycogen was very low, reflecting slow glycogen turnover rates during daily feeding regimes and consistent with previous observations of low glycogen turnover rates in seabass under these conditions (Viegas et al. 2015; Viegas et al. 2012).

4. Discussion:

Our experimental results indicate that an intraperitoneal glycerol bolus is readily utilized as a gluconeogenic substrate by juvenile seabass, contributing ~20 and 50% of systemic glucose appearance in fed and fasted conditions, respectively. Moreover, glycerol also replenished the hepatic glycogen reserves of 21-day fasted fish. To the extent that this activity is sparing the gluconeogenic catabolism of dietary AA, glicerol utilization could have a significant impact on waste ammonia generation. While this potentially beneficial aspect of glycerol metabolism has not been yet investigated in fish rearing, replacement of 5-15% of fish-feed components by glycerol appears to be well tolerated by many different species including carnivorous fish. In cultured channel catfish (*Ictalurus punctatus*), substitution of 10% feed dry weight by glycerol had no significant effects on growth and fillet quality (Li et al. 2010). Moreover, glycerol was well retained within feed pellets and efficiently ingested (Li et al. 2010). In mature gilthead seabream *(Sparus aurata*), supplementation of standard feed with 5% glycerol increased muscle glycogen and ATP levels over fish fed on standard feed alone, indicating a positive contribution to whole body carbohydrate and energy reserves (Silva et al. 2012). To date, glycerol utilization by farmed fish has been studied most closely in tilapia, a widely cultured omnivorous fish species. In Nile tilapia fingerlings, complete replacement of dietary maize (17% of feed weight) by glycerol was well tolerated (Moesch et al. 2016) while in another study, replacement of wheat bran with glycerol representing up to 15% of feed weight also sustained normal growth rates (da Costa et al. 2017). To our knowledge, glycerol utilization by seabass has not been previously reported.

While metabolism of circulating glycerol derived either endogenously via triglyceride lipolysis or exogenously from a glycerol load has been well studied in humans and other mammalian species (Baba et al. 1995; Bergman et al. 1968; Cohen et al. 1979; Jin et al. 2014; Jin et al. 2016; Landau et al. 1996), to date there have been relatively few reports of glycerol metabolism in fish. Endogenous glycerol production and synthesis activities have been indirectly inferred from studies of triglyceride turnover using labeled triglyceride and VLDL (Magnoni et al. 2008) and hepatic triglyceride biosynthesis using deuterated water (Viegas et al. 2016). As in mammals, it appears that triglyceride turnover rates are considerably in excess of fatty acid oxidation in rainbow trout (Magnoni et al. 2008). In seabass, turnover of the hepatic triglyceride glycerol moiety far exceeded that of the fatty acid components (Viegas et al. 2016). Both sets of observations are consistent with fatty acid-triglyceride cycling activity and imply the operation of a corresponding cycle of endogenous glycerol clearance and de novo glycerol-3-P synthesis. Since the canonical pathway for systemic glycerol disposal is hepatic conversion to glucose via glycerol kinase and glycerol-3-phosphate dehydrogenase followed by gluconeogenesis, it follows that this activity is likely to be constitutive in fish as well as in mammals. This, coupled with the presence of intestinal aquaporin transporters that facilitate glycerol absorption (Engelund et al. 2013; Tingaud-Sequeira et al. 2010) may explain the high rates of feed glycerol utilization that have been measured to date in various fish species (Balen et al. 2014; da Costa et al. 2017).

In rainbow trout, glycerol kinase activity was measured in superfused liver slices while radiolabeling of glycogen and lipids from ^{14}C-glycerol was also detected *in vitro* (Lech 1970). A portion of the ^{14}C-glycerol was recovered in CO_2, indicating that a fraction of glycerol carbons had been incorporated into oxidative metabolism. This is consistent with our observations showing that a portion of the glycerol load was metabolized *via* the Krebs cycle. In a study of oral [U-^{14}C]glycerol utilization by 12-hour fasted juvenile tilapia, radioactivity was recovered in both CO_2 and muscle protein (da Costa et al. 2017). These data are also consistent with entry of glycerol carbon label into

the Krebs cycle where not only can it be oxidized to CO_2 but can also be incorporated into aspartate, glutamate and alanine via transaminase-mediated exchanges with Krebs cycle intermediates and pyruvate. However, the majority of radioactivity in both liver and muscle was recovered from a so-called nonprotein, non-lipid fraction (NPNL) which presumably included glucose and glycogen metabolites (da Costa et al. 2017). Their liver observations are consistent with the high contribution of glycerol to liver glycogen observed for the fasted fish in our study. Muscle NPNL labeling likely includes muscle glycogen generated from labeled circulating glucose that had in turn been derived from hepatic gluconeogenesis of the labeled glycerol.

In fasted fish, a significant excess of [1,2-$^{13}C_2$] over the [5,6-$^{13}C_2$] isotopomer was observed in both glucose and glycogen. Similar observations were reported for plasma glucose ^{13}C-isotopomers from both fasted and fed rats that were intraperitoneally administered with [U-$^{13}C_3$]glycerol (Jin et al. 2014). This isotopomer inequality is explained by pentose phosphate pathway (PPP) activity and provides a basis for estimating PPP fluxes, provided that [2,3-$^{13}C_2$] and [4,5-$^{13}C_2$]glucose or glycogen isotopomers can also be measured (Jin et al. 2014). In our experiments, [2,3-$^{13}C_2$] and [4,5-$^{13}C_2$]glucose isotopomers could not be reliably measured due to insufficient signal-to-noise, hence we could not confidently estimate PPP fluxes from plasma glucose analysis under our experimental conditions. In the fasted glycogen spectra where [2,3-$^{13}C_2$] and [4,5-$^{13}C_2$]glycogen isotopomers were quantified with high confidence, PPP flux as a fraction of glycerol gluconeogenesis was estimated according to the method of Jin et al. (Jin et al. 2014) and was found to be not significantly different from zero (data not shown).

In our study, the glycerol load was supra-physiological and was administered intraperitoneally hence our observations may not reflect the metabolism of glycerol added to fish-feed. We did not measure the fraction of un-metabolized glycerol that was cleared into the tank water. Our estimates of fractional glycerol utilization for glucose and glycogen synthesis did not take into account the possible dilution of the glycerol tracer by exchange with unlabeled triglyceride glycerol

mediated by triglyceride-fatty acid cycling. Analysis of the plasma [U-$^{13}C_3$]glycerol isotopomer signals from both fasted and fed fish indicated that the enrichment levels (27 ± 2% for both conditions) were equivalent to the 25%-enriched glycerol load indicating no significant dilution under our study conditions. However, a smaller glycerol load than the one used in our study and/or longer duration of labeled glycerol administration is likely to be more susceptible to such dilution. For estimating the fraction of hepatic glucose and glycogen that was synthesized from glycerol via the Krebs cycle, our assumptions of anaplerotic and oxidative hepatic Krebs cycle fluxes have not been validated in any fish species. Finally, since Cori cycling of [1,2,3-$^{13}C_3$] and [4,5,6-$^{13}C_3$]glucose also generates [1,2-$^{13}C_2$] and [5,6-$^{13}C_2$]Glc-6-P isotopomers[1] (Coelho et al. 2015; Perdigoto et al. 2003; Rito et al. 2017), there is uncertainty about the true extent of hepatic glycerol metabolism through the Krebs cycle.

In conclusion, we present evidence for extensive gluconeogenic utilization of exogenous glycerol by juvenile seabass under both fasted and feeding conditions. Our studies suggest that glycerol can effectively compete with other endogenous gluconeogenic precursors such as AA for carbohydrate biosynthesis thereby potentially reducing AA catabolism and the resulting generation of nitrogenous waste. These observations open a new perspective on the beneficial effects of glycerol as a fish-feed supplement for carnivorous fish such as seabass.

Acknowledgements:

Structural funding for the Center for Neuroscience and Cell Biology, Centre for Functional Ecology, and the UC-NMR facility is supported in part by FEDER – European Regional Development Fund, within the PT2020 Partnership Agreement, the COMPETE 2020 Programme within the project UID/BIA/04004/2013, and the Portuguese Foundation for Science and Technology (FCT/MEC) through grants PTDC/EBB-BIO/098111/2008, EXCL/DTP-PIC/0069/2012, PTDC/CVT-NUT/2851/2014, PEst-C/SAU/LA0001/2011; REEQ/481/QUI/2006, RECI/QEQ-QFI/0168/2012,

[1] [1,2,3-$^{13}C_3$],[4,5,6-$^{13}C_3$]glucose → → [1,2,3-$^{13}C_3$]pyruvate/lactate in muscle → → 0.5 [1,2-$^{13}C_2$], [5,6-$^{13}C_2$]glucose + 0.5 [1,2,3-$^{13}C_3$],[4,5,6-$^{13}C_3$]glucose in liver.

CENTRO-07-CT62-FEDER-002012, and Rede Nacional de Ressonância Magnética Nuclear. Authors also acknowledge funding through a Ph.D scholarship to João Rito (SFRH/BD/87056/2012) and Postdoctoral fellowship to Ivan Viegas (SFRH/BPD/90032/2012) from FCT and to Eng. Canas for providing the European seabass for the experiments. The authors also acknowledge financial support in the form of research grants from MEC (Spain) (AGL2012-33305 and AGL2016-78124-R; co-funded by the ERDF).

References

Arif, M., Abd El-Hack, M.E., Hayat, Z., Sohail, S., Saeed, M., Alagawany, M., 2017. The beneficial uses of glycerin as an alternative energy source in poultry diets. Worlds Poultry Science Journal. 73, 136-144.

Baba, H., Zhang, X.J., Wolfe, R.R., 1995. Glycerol gluconeogenesis in fasting humans. Nutrition. 11, 149-153.

Balen, R.E., Tetu, P.N., Bombardelli, R.A., Pozza, P.C., Meurer, F., 2014. Digestible energy of crude glycerol for Pacu and Silver catfish. Ciencia Rural 44, 1448-1451.

Bergman, E.N., Starr, D.J., Reulein, S.S., Jr., 1968. Glycerol metabolism and gluconeogenesis in the normal and hypoglycemic ketonic sheep. American Journal of Physiology 215, 874-880.

Bever, K., Chenoweth, M., Dunn, A., 1977. Glucose turnover in kelp bass (Paralabrax-sp) - in vivo studies with [6-^{3}H,6-^{14}C]glucose. American Journal of Physiology 232, R66-R72.

Coelho, M., Nunes, P., Mendes, V.M., Manadas, B., Heerschap, A., Jones, J.G., 2015. Effect of global ATGL knockout on murine fasting glucose kinetics. Journal of Diabetes Research Article ID 542029, doi:10.1155/2015/542029.

Cohen, S.M., Ogawa, S., Shulman, R.G., 1979. ^{13}C NMR studies of gluconeogenesis in rat liver cells: utilization of labeled glycerol by cells from euthyroid and hyperthyroid rats.

Proceedings of the National Academy of Sciences of the United States of America 76, 1603-1609.

da Costa, D.V., Dias, J., Colen, R., Rosa, P.V., Engrola, S., 2017. Partition and metabolic fate of dietary glycerol in muscles and liver of juvenile tilapia. Archives of Animal Nutrition 71, 165-174.

Engelund, M.B., Chauvigne, F., Christensen, B.M., Finn, R.N., Cerda, J., Madsen, S.S., 2013. Differential expression and novel permeability properties of three aquaporin 8 paralogs from seawater-challenged Atlantic salmon smolts. Journal of Experimental Biology. 216, 3873-3885.

FEAP – Federation of European Aquaculture Producers, 2017. European Aquaculture Report 2008-2016. http://www.feap.info .

Gonçalves, L.U., da Silva Cerozi, B., Silva, T.S.C., Zanon, R.B., Cyrino, J.E.P., 2015. Crude glycerin as dietary energy source for Nile tilapia. Aquaculture 437, 230-234.

Good, C.A., Kramer, H., Somogyi, M., 1933. The determination of glycogen. J Biol Chem. 100, 485-491.

Hers, H.G., 1976. The control of glycogen metabolism in the liver. Annual Review of Biochemistry. 45, 167-189.

Jin, E.S., Sherry, A.D., Malloy, C.R., 2014. Interaction between the pentose phosphate pathway and gluconeogenesis from glycerol in the liver. Journal of Biological Chemistry 289, 32593-32603.

Jin, E.S., Sherry, A.D., Malloy, C.R., 2016. An oral load of [U-$^{13}C_3$]glycerol and blood NMR analysis detect fatty acid esterification, pentose phosphate pathway, and glycerol metabolism through the tricarboxylic acid cycle in human liver. Journal of Biological Chemistry 291, 19031-19041.

Kosuga, M., Henderson-MacLennan, N.K., Zhang, Y.-H., Huang, B.-L., Dipple, K.M., McCabe, E.R., 2011. Glycerol homeostasis and metabolism in glycerol kinase carrier mice. Molecular Genetics and Metabolism 103, 297-299.

Krebs, H., 1964. Gluconeogenesis. Proceedings of the Royal Society of London. Series B, Biological Sciences. 159, 545-564.

Landau, B.R., Wahren, J., Previs, S.F., Ekberg, K., Chandramouli, V., Brunengraber, H., 1996. Glycerol production and utilization in humans: sites and quantitation. American Journal of Physiology 271, E1110-E1117.

Lech, J.J., 1970. Glycerol kinase and glycerol utilization in trout (salmo-gairdneri) liver. Comparative Biochemistry and Physiology. 34, 117-124.

Lee, S.Y., Lee, S.M., Cho, Y.B., Kam, D.K., Lee, S.C., Kim, C.H., Seo, S., 2011. Glycerol as a feed supplement for ruminants: In vitro fermentation characteristics and methane production. Animal Feed Science and Technology 166-67, 269-274.

Li, M.H., Minchew, C.D., Oberle, D.F., Robinson, E.H., 2010. Evaluation of glycerol from biodiesel production as a feed ingredient for channel catfish, Ictalurus punctatus. Journal of the World Aquaculture Society 41, 130-136.

Lin, E., 1977. Glycerol utilization and its regulation in mammals. Annual Review of Biochemistry. 46, 765-795.

Magnoni, L., Vaillancourt, E., Weber, J.-M., 2008. High resting triacylglycerol turnover of rainbow trout exceeds the energy requirements of endurance swimming. American Journal of Physiology 295, R309-R315.

Meurer, F., Franzen, A., Piovesan, P., Rossato, K.A., Dos Santos, L.D., 2012. Apparent energy digestibility of glycerol from biodiesel production for Nile tilapia (Oreochromis niloticus, Linnaeus 1758). Aquaculture Research 43, 1734-1737.

Moesch, A., Meurer, F., Zadinelo, I.V., Carneiro, W.F., Rosa da Silva, L.C., dos Santos, L.D., 2016. Growth, body composition and hepatopancreas morphology of Nile tilapia fingerlings fed crude glycerol as a replacement for maize in diets. Animal Feed Science and Technology 219, 122-131.

Perdigoto, R., Rodrigues, T.B., Furtado, A.L., Porto, A., Geraldes, C.F., Jones, J.G., 2003. Integration of [U-^{13}C]glucose and $^{2}H_2O$ for quantification of hepatic glucose production and gluconeogenesis. NMR in Biomedicine 16, 189-198.

Peres, H., Oliva-Teles, A., 1999. Influence of temperature on protein utilization in juvenile European seabass (Dicentrarchus labrax). Aquaculture 170, 337-348.

Peres, H., Oliva-Teles, A., 2005. Protein and energy metabolism of European seabass (Dicentrarchus labrax) juveniles and estimation of maintenance requirements. Fish Physiology and Biochemistry 31, 23-31.

Rito, J., Viegas, I., Pardal, M.A., Jones, J.G., 2017. Evidence of extensive plasma glucose recycling following a glucose load in seabass. Comparative Biochemistry and Physiology Part A: Molecular & Integrative Physiology. 211, 41-48.

Silva, T.S., Matos, E., Cordeiro, O.D., Colen, R., Wulff, T., Sampaio, E., Sousa, V., Valente, L.M.P., Gonçalves, A., Silva, J.M.G., Bandarra, N., Nunes, M.L., Dinis, M.T., Dias, J., Jessen, F., Rodrigues, P.M., 2012. Dietary tools to modulate glycogen storage in gilthead seabream muscle: glycerol supplementation. Journal of Agricultural and Food Chemistry 60, 10613-10624.

Tingaud-Sequeira, A., Calusinska, M., Finn, R.N., Chauvigne, F., Lozano, J., Cerda, J., 2010. The zebrafish genome encodes the largest vertebrate repertoire of functional aquaporins with dual paralogy and substrate specificities similar to mammals. BMC Evolutionary Biology. 10, 38, doi.org/10.1186/1471-2148-10-38.

Viegas, I., Jarak, I., Rito, J., Carvalho, R.A., Meton, I., Pardal, M.A., Baanante, I.V., Jones, J.G., 2016. Effects of dietary carbohydrate on hepatic de novo lipogenesis in European seabass (Dicentrarchus labrax L.). Journal of Lipid Research. 57, 1264-1272.

Viegas, I., Rito, J., Jarak, I., Leston, S., Carvalho, R.A., Metón, I., Pardal, M.A., Baanante, I.V., Jones, J.G., 2012. Hepatic glycogen synthesis in farmed European seabass (Dicentrarchus labrax L.) is dominated by indirect pathway fluxes. Comparative Biochemistry and Physiology a-Molecular & Integrative Physiology. 163, 22-29.

Viegas, I., Rito, J., Jarak, I., Leston, S., Caballero-Solares, A., Meton, I., Pardal, M.A., Baanante, I.V., Jones, J.G., 2015. Contribution of dietary starch to hepatic and systemic carbohydrate fluxes in European seabass (Dicentrarchus labrax L.). British Journal of Nutrition. 113, 1345-1354.

Footnote:

[a][1,2,3-$^{13}C_3$],[4,5,6-$^{13}C_3$]glucose → → [1,2,3-$^{13}C_3$]pyruvate/lactate in muscle → → 0.5 [1,2-$^{13}C_2$], [5,6-$^{13}C_2$]glucose + 0.5 [1,2,3-$^{13}C_3$],[4,5,6-$^{13}C_3$]glucose in liver.

Figure Legends:

Figure 1: Schematic of glucose-6-phosphate (Glc-6-P) ^{13}C-isotopomer classes **A-D** generated from the gluconeogenic metabolism of glycerol enriched with [U-$^{13}C_3$]glycerol. Selected metabolite carbon skeletons are represented by connected circles, where filled circles represent ^{13}C atoms and unfilled circles represent ^{12}C atoms. Conversion of [U-$^{13}C_3$]glycerol to form [1,2,3-$^{13}C_3$]triose-P followed by gluconeogenesis generates isotopomers **A**, represented by black filled circles. Passage of triose-P carbons into and out of the Krebs cycle via pyruvate carboxylase and PEP-carboxykinase, represented by the dashed line, converts a portion of [1,2,3-$^{13}C_3$]triose-P to [2,3-$^{13}C_2$]triose-P which in turn generate Glc-6-P isotopomers **B**, represented by dark grey filled circles. Further randomization of ^{13}C through a complete turn of the Krebs cycle generates [1,2-$^{13}C_2$]triose-P resulting in Glc-6-P isotopomers **C**, represented by light gray filled circles. Unlabeled Glc-6-P formed from triose-P intermediates that are not enriched from [U-$^{13}C_3$]glycerol is also shown (**D**). For simplicity, some metabolic intermediates are omitted. Also, formation of Glc-6-P isotopomers from the condensation of two labeled triose-P precursors is assumed to be negligible.

Figure 2: ^{1}H NMR spectra of MAG obtained from pooled blood samples of 3 fish administered with a 2 g.kg^{-1} glycerol load enriched to 25% with [U-$^{13}C_3$]glycerol (**a**) and pooled blood samples of 3 fish administered with saline (**b**). The numbers above each hydrogen resonance indicates its position in the hexose moiety of MAG. For the spectrum derived from [U-$^{13}C_3$]glycerol-injected fish, signals derived from ^{1}H-^{13}C coupling of position 1 hydrogen and ^{13}C are indicated as ^{13}C while the signal from ^{1}H bound to ^{12}C is indicated as ^{12}C. Also shown are the resolvable plasma glycerol 1_R, 3_S and position 2 signals.

Figure 3: ^{13}C NMR spectra of MAG obtained from pooled blood samples of 3 fish administered with a 2g.kg^{-1} glycerol load enriched to 25% with [U-$^{13}C_3$]glycerol (**a**) and pooled blood samples of

3 fish administered with saline (**b**). The numbers above each carbon resonance indicates its position in the hexose moiety of MAG. The two natural-abundance ^{13}C-signals from the acetonide methyl carbons of MAG are also indicated (**A**). The carbon 2 and carbon 5 resonances of spectrum (a) are shown in expanded view to illustrate their multiplet components. **Q** = quartet; **D12** = doublet from coupling between MAG ^{13}C1 and ^{13}C2, **D56** = doublet from coupling between MAG ^{13}C5 and ^{13}C6; **S** = natural abundance singlet. Also indicated are the ^{13}C signals from glycerol carbon 2 (**Gly 2**) and carbons 1 and 3 (**Gly 1,3**).

Figure 4: ^{13}C NMR carbon 2 multiplets of MAG derived from plasma glucose and liver glycogen of fasted fish (top) and fed fish (bottom) following administration with [U-$^{13}C_3$]glycerol. The multiplet components are **Q** = quartet; **D12** = doublet from coupling between MAG ^{13}C1 and ^{13}C2, **D23** = doublet from coupling between MAG ^{13}C2 and ^{13}C3; **S** = natural abundance singlet. Above the spectra, the relationship between the multiplet components and isotopomer groups **A-D** is shown.

Table 1: Plasma glucose and glycerol levels for fed and 21-day fasted seabass saline- (Control) and glycerol-injected immediately before (0 hours) and 48 hours after the [U-^{13}C]glucose load and final liver glycogen levels

	Control		Glycerol-injected	
	Fed	Fasted	Fed	Fasted
Plasma glucose (mM)				
0 hours	6.7 ± 0.77	6.1 ± 1.66	8.9 ± 2.87	5.6 ± 1.66
48 hours	4.6 ± 1.42	8.8 ± 1.59	9.3 ± 0.46	11.0 ± 2.79
Final liver glycogen (g.100g^{-1} liver)	10.5 ± 0.22 *	2.7 ± 0.91 †	8.0 ± 1.21	7.7 ± 0.45
Plasma glycerol (mM)				
0 hours	0.04 ± 0.00	0.05 ± 0.01	0.09 ± 0.01 Ψ	0.08 ± 0.02 Ψ
48 hours	0.04 ± 0.01	0.07 ± 0.01	1.11 ± 0.03	1.02 ± 0.08

Significant differences in glycogen between fed and fasted control groups are indicated by asterisks (*t*-test, * $P< 0.001$). Significant differences in glycogen between control and glycerol-injected fasted groups are indicated by † (*t*-test, $P< 0.005$). Significant differences in plasma glycerol between 0h and 48h glycerol-injected fed or fasted groups are indicated by Ψ (*t*-test, Ψ $P< 0.0001$).

Table 2: Percent abundances of nearest-neighbor ^{13}C-isotopomers of positions 2 and 5 of pooled glucose and glycogen samples in fasted and fed juvenile seabass administered with 2 g.kg^{-1} [U-$^{13}C_3$]glycerol. For each metabolite and condition, *n* refers to the number of pooled samples.

	Position 2 Isotopomers					**Position 5 Isotopomers**			
	[1,2,3-$^{13}C_3$]-	[1,2-$^{13}C_2$]-	[2,3-$^{13}C_2$]-	[2-^{13}C]-		[4,5,6-$^{13}C_3$]-	[5,6-$^{13}C_2$]-	[4,5-$^{13}C_2$]-	[5-^{13}C]-
Isotopomer designation	**A**	**B**	**C**	**D**		**A**	**B**	**C**	**D**
Fasted Glucose (*n*=4)	9.4 ± 0.7 *	1.2 ± 0.1 ǂ	N.Q.	1.1		8.2 ± 0.4 *	0.7 ± 0.2 Ψ	N.Q.	1.1
Fasted Glycogen (*n*=8)	9.3 ± 0.8 †	1.6 ± 0.1 ǂǂ	0.6 ± 0.1	1.1		7.3 ± 0.7 †	1.1 ± 0.1	0.4 ± 0.1	1.1
Fed Glucose (*n*=6)	2.5 ± 0.4	1.2 ± 0.2	N.Q.	1.1		3.0 ± 0.4	0.8 ± 0.2	N.Q.	1.1
Fed Glycogen (*n*=7)	0.3 ± 0.1	0.2 ± 0.1 †	N.Q.	1.1		0.3 ± 0.1	0.1 ± 0.0 †	N.Q.	1.1

N.Q. not quantifiable – below the limit of quantification (isotopomer signal-to-noise ratio < 5:1)

Significant differences between fasted and fed glucose are indicated by asterisks (t-test, $P< 0.0001$). Significant differences between fasted and fed glycogen are indicated by † (t-test, $P< 0.0001$). Significant differences between fasted [5,6-$^{13}C_3$]glucose and glycogen isotopomers are

indicated by $^{\Psi}$ (*t*-test, $P< 0.05$). Significant differences between [1,2-$^{13}C_3$]- and [5,6-$^{13}C_3$]glucose isotopomers are indicated by ‡ (t-test, $P< 0.05$) and differences between [1,2-$^{13}C_3$]- and [5,6-$^{13}C_3$]glycogen isotopomers by ‡‡ (t-test, $P< 0.01$).

Table 3: Fractional contribution of glycerol load carbons to circulating glucose and hepatic glycogen in fasted and fed juvenile seabass administered with 2 g.kg^{-1} [U-$^{13}C_3$]glycerol. Contributions are resolved into linear gluconeogenesis and glucogneogenesis via the Krebs cycle.

	Fractional contribution of [U-$^{13}C_3$]glycerol load to glucose and glycogen appearance (%)		
	All pathways	Linear gluconeogenesis	Gluconeogenesis via Krebs cycle
Fasted Glucose	47 ± 3 *	40 ± 3 **	7 ± 2
Fasted Glycogen	40 ± 3	28 ± 3 ^{ǂ}	12 ± 1 ^{ǂ}
Fed Glucose	17 ± 3 ^{ΨΨ}	10 ± 2 ^{ΨΨΨ}	6 ± 2 ^{Ψ}
Fed Glycogen	3 ± 1 †	2 ± 1 †	1 ± 0 †

Significant differences between fasted and fed glucose are indicated by asterisks (*t*-test, * $P< 0.0005$; ** $P< 0.0001$). Significant differences between fasted and fed glycogen are indicated by † (*t*-test, $P< 0.0001$). Significant differences between glucose and glycogen fasted are indicated by ^{ǂ} (*t*-test, $P< 0.05$). Significant differences between glucose and glycogen fed are indicated by ^{Ψ} (*t*-test, ^{Ψ} $P< 0.005$; ^{ΨΨ} $P< 0.001$; ^{ΨΨΨ} $P< 0.0005$.

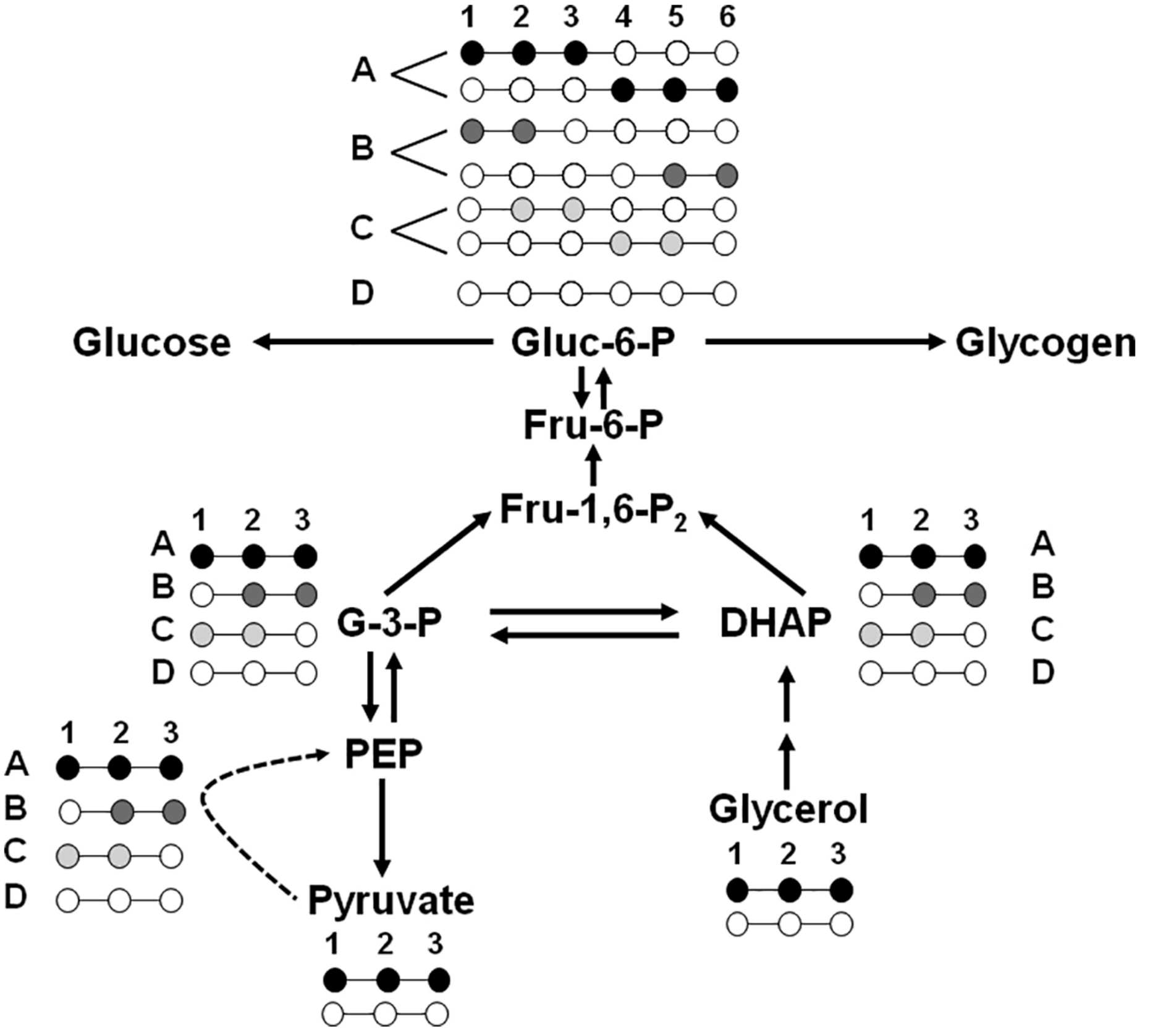
1 2 3 4 5 6
A
B
C
D
Glucose
Gluc-6-P
Glycogen
Fru-6-P
Fru-1,6-P2
1 2 3
A
B
C
D
G-3-P
DHAP
PEP
Glycerol
Pyruvate

Figure 1

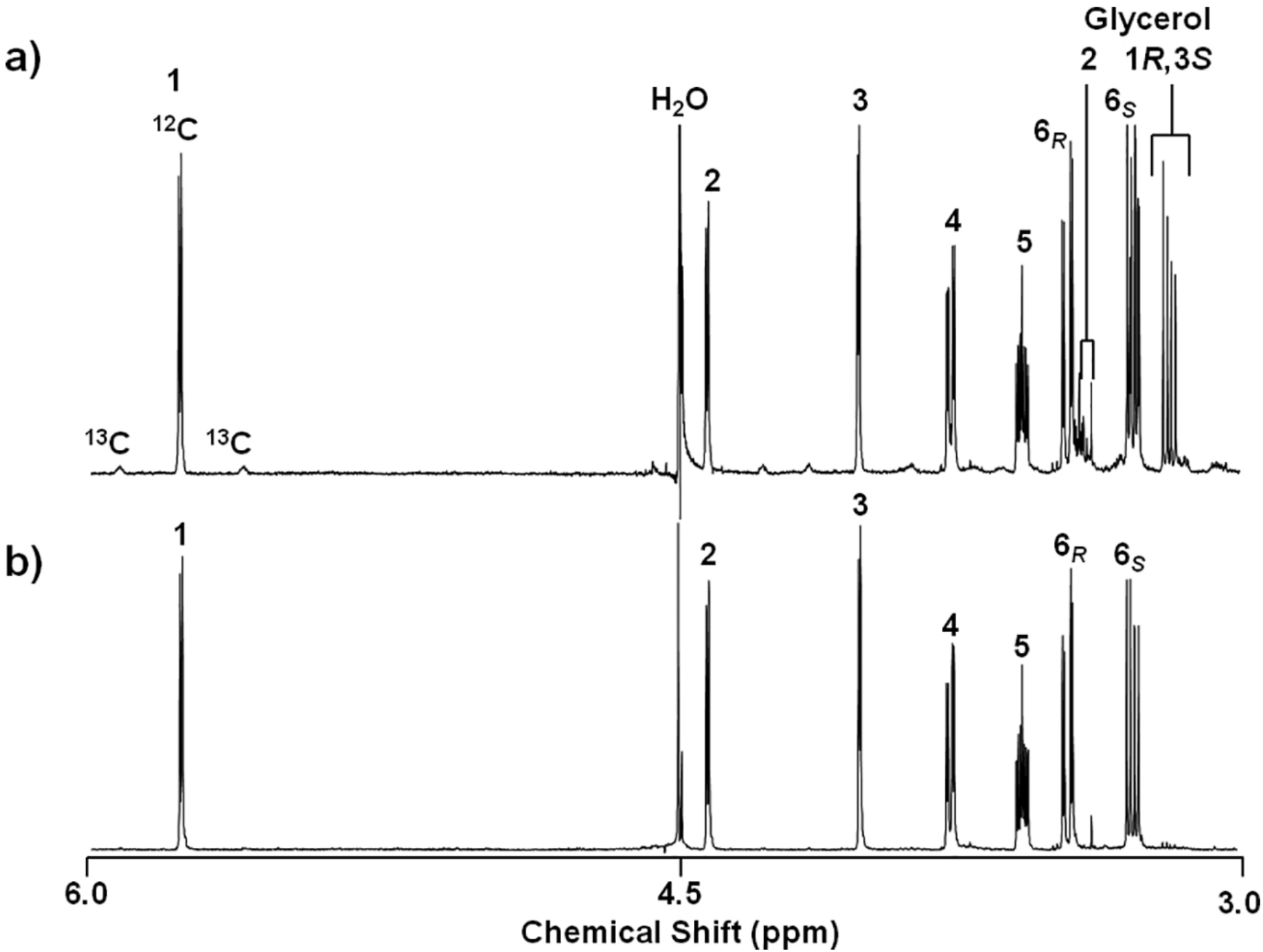
a)
b)
1
^{12}C
^{13}C
^{13}C
H_2O
2
3
4
5
6_R
6_S
Glycerol
2
1R,3S
6.0
4.5
3.0
Chemical Shift (ppm)

Figure 2

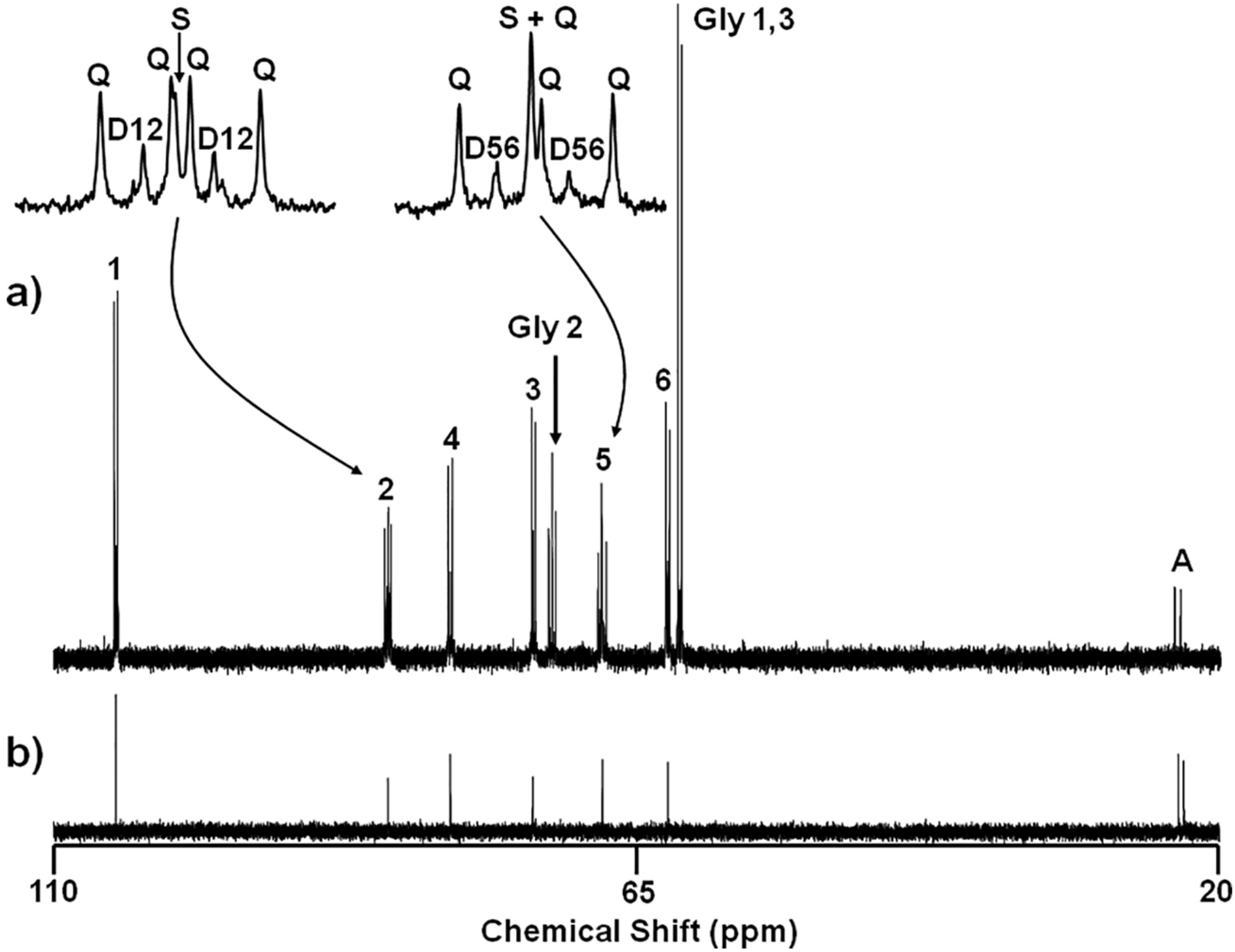
S
Q
Q
Q
Q
D12
D12
S + Q
Q
Q
Q
D56
D56
Gly 1,3
a)
1
Gly 2
3
6
4
5
2
A
b)
110
65
20
Chemical Shift (ppm)

Figure 3

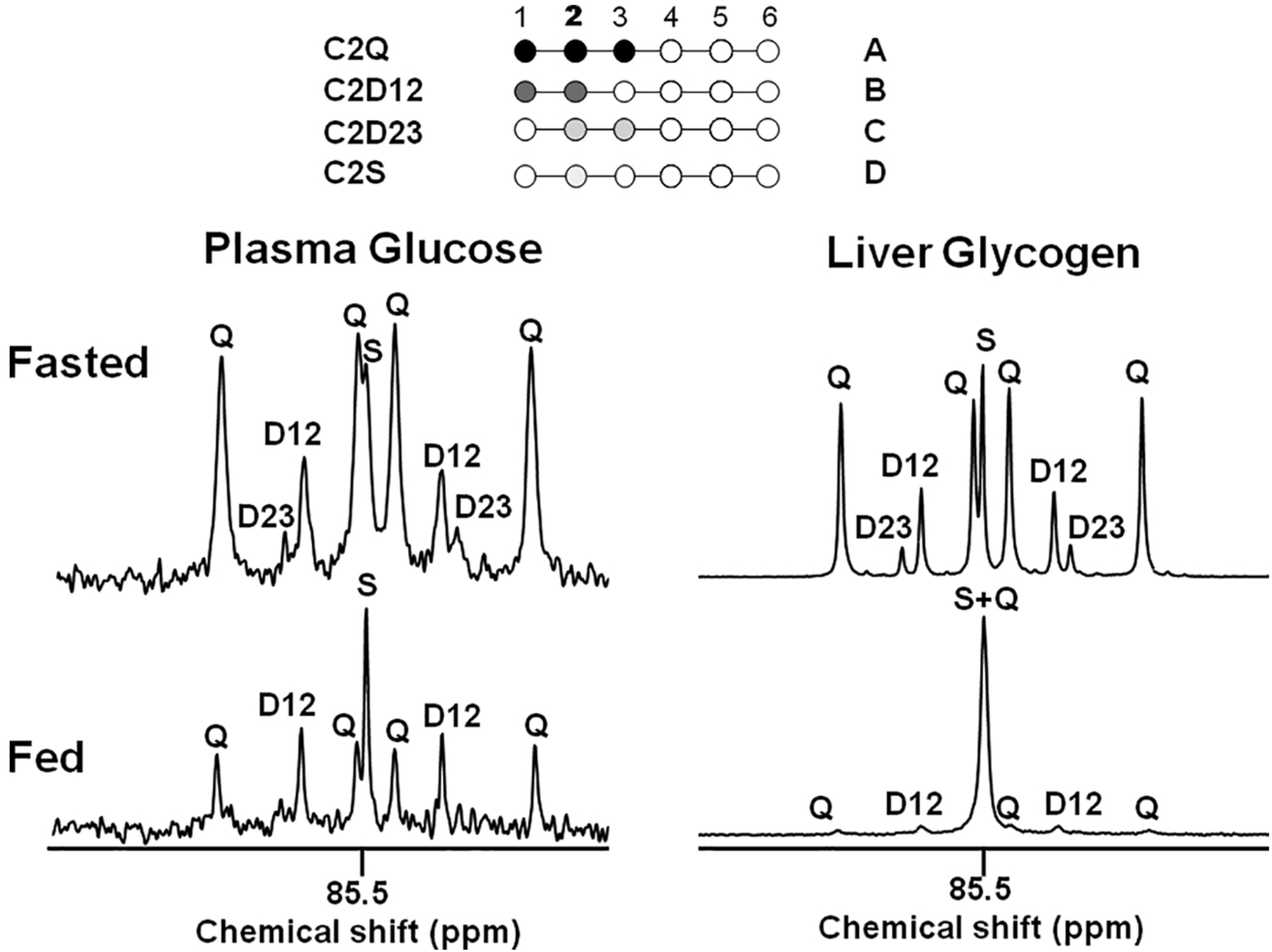
1 2 3 4 5 6
C2Q
C2D12
C2D23
C2S
A
B
C
D
Plasma Glucose
Liver Glycogen
Fasted
Fed
Q
S
D12
D23
S+Q
85.5
Chemical shift (ppm)

Figure 4